Proceedings of the ASME 2023
International Design Engineering Technical Conferences and
Computers and Information in Engineering Conference
IDETC/CIE2023
August 20-23, 2023, Boston, Massachusetts

DETC2023-117322

MACHINE LEARNING BASED DEFLECTION PREDICTION AND INVERSE DESIGN FOR DISCRETE VARIABLE STIFFNESS UNITS

Jiaming Fu[1†], Qianyu Guo[1†], Dongming Gan[1*]

[1]Polytechnic Institute, Purdue University, West Lafayette, IN47907, US

ABSTRACT

Large deflection modeling is a crucial field of study in the analysis and design of compliant mechanisms (CM). The aim of this research paper is to propose a machine learning approach for predicting the deflection of discrete variable stiffness units (DSUs) that cover a range from small to large deflections. The primary structure of a DSU consists of a parallel guide beam with a hollow cavity that can change stiffness discretely by inserting or extracting a solid block. The principle is based on changing the cross-sectional area properties of the hollow section. Prior to model training, a large volume of data was collected using finite element analysis (FEA) under different loads and various dimensional parameters. Additionally, we present three widely used machine learning-based models for predicting beam deflection, taking into account prediction accuracy and speed. Several experiments are conducted to evaluate the performance of the models. The optimal machine learning model can achieve a 1.97% error compared to FEA. Furthermore, the model was employed in a practical application for inverse design, with various cases presented depending on the number of solved variables. This method provides a unique perspective for studying the modeling of compliant mechanisms and may be extended to other mechanical mechanisms.

Keywords: large deflection modeling, discrete variable stiffness, machine learning, parallel beam, stiffness modeling, compliant mechanism

1. INTRODUCTION

Collaborative robots are becoming increasingly popular in shared workspaces within the industry due to the limitations of conventional industrial robots that require enclosures for safety reasons [1]. To ensure human safety during joint working operations, two types of safety measures, active and passive, are usually employed [2]. An instance of active safety is the application of 3D vision [3] to detect human proximity, causing the robot to slow down or halt. Passive safety is typically achieved by torque sensors that detect collisions, which immediately stop the robot at the joint [4].

However, intrinsic safety methods are also necessary to address potentially dangerous situations arising from electronic module failure [5]. One viable approach involves the use of soft materials to envelop the robotic arm [6], reducing the impact of collisions. Alternatively, the safety issue can be addressed through mechanical design approaches by adopting compliant mechanisms [7].

In order to compute the large deflection of flexible beams, which is the crucial component of compliant mechanisms, it requires efficient and accurate analysis methods . Three common methods for analyzing beam deflection include pseudo-rigid-body methods (PRBM) [8], beam-constraint-model methods (BCM) [9], chained beam-constraint-model[10], and finite element methods (FEM). Howell and Midha proposed a method for approximating the deflection path of end-loaded large-deflection cantilever beams, which involves the use of a physical model based on the PRBM. The values for key parameters have been determined using elliptic integral equations and verified with a numerical finite element algorithm in their paper. This method simplifies complex problems associated with geometric nonlinearity in large-deflection beams.

In [9], Su proposed the PRB 3R model approximates cantilever beam deflection and solves large deflection beam equations through numerical integration. A comprehensive tip deflection atlas is obtained, and a three-dimensional search

† These authors contributed equally.
* Please address all correspondence to this author, dgan@purdue.edu

routine is developed to optimize the PRB 3R model. Error analysis shows that the PRB 3R model has a smaller approximation error than the PRB 1R model, and benefits include the independence of external loads, small approximation error for large deflection beams, and simpler constraint equations.

In addition to the numerical simulations described above, the FEA can also evaluate the mechanical performance of a compliant mechanism. However, there are still several challenges that need to be addressed in this method. Because utilizing FEA models is high computational cost, difficult to impose more physical and geometric constraints, and requires non-measurable variables and suppositions that must be validated through experimental testing, which is a costly and intricate process [11]. To overcome those constraints, the authors utilize the Machine Learning (ML) algorithm to identify and reconstruct intricate internal correlations among multiple variables using extensive datasets collected via FEA.

Despite a lot of conventional methods of calculation and analysis that have been proposed and widely used, methods based on machine learning are increasingly being implemented in the field of mechanical engineering. For instance, [12] proposed a machine learning-based algorithm to progressively optimize the vehicle's thin-walled structure in order to increase its crashworthiness. Using the K-means algorithm, the optimal number of clusters was determined during the parametric design phase. In [13], computational intelligence and machine learning techniques were utilized to estimate the static properties of specific fluidic muscles, and a high prediction accuracy was achieved. In addition, [14] introduced and compared various machine learning models for predicting the deformation and shape of 2D cantilever beams.

In this work, we propose to apply machine learning algorithms to estimate the degree of deflection of discrete variable stiffness units, while achieving high prediction accuracy and speed. We introduce the three most popular ML models Support Vector Machine (SVM) [11], Gaussian process regression (GPR) [15][16], and Multilayer Perceptron (MLP) [17]. By comparing the obtained Root Mean Square Error (RMSE) and prediction speed of the three models, we are able to select the optimal algorithm that could be applied to the prediction of DSU deflection.

In this paper, a novel machine learning approach is proposed for predicting the deflection of discrete variable stiffness units (DSUs), which are made of a parallel guide beam with a hollow cavity that can change stiffness by inserting or extracting a solid block. Section 2 of this paper outlines the mechanical design, parameters, data collection, and machine learning methods. Subsequently, the results and analysis of the ML model, analytical model, and FEA are presented in section 3. In section 4, a comparison is made between the inverse design of the ML model and the analytical model with different variables. Finally, section 5 concludes the study.

2. PRINCIPLE AND MODELING

2.1 Principle of stiffness variation

The adjustment of mechanism stiffness can be achieved through two fundamental methods, namely, continuous and discrete. Fig. 1(a) displays a hollow parallel guided beam with a rectangular cavity housing a solid block. By altering the position of the block within the cavity, the stiffness of the beam can be continuously changed. As the block approaches the cavity's center, the stiffness increases, while it decreases as the block approaches the cavity's ends. On the other hand, the DSU depicted in Fig. 1(b) utilizes a discrete approach by moving the solid block along the vertical direction of the beam's length. The system offers two stiffness levels, with the block inserted in the cavity with a larger stiffness, called on mode, and being pulled out of the cavity with a lower stiffness, called off mode. The variation of the beam's stiffness is attributed to changing the cross-sectional area properties of its hollow section [18].

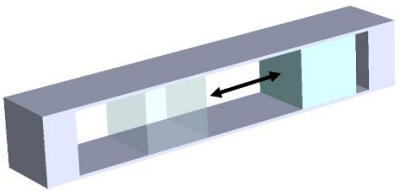

(a) CONTINUOUS STIFFNESS VARIATION

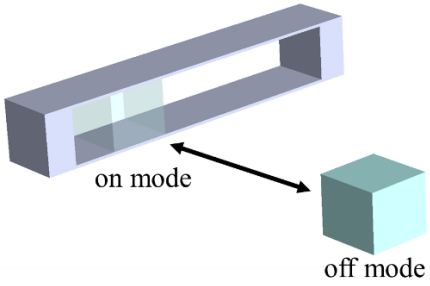

(b) DISCRETE STIFFNESS VARIATION

FIGURE 1: STIFFNESS CHANGE PRINCIPLES

2.2 Analytical stiffness model

In [19], we proposed a linear stiffness model for the DSU. This model is suitable for small and medium deflections up to 10% relative to the beam length with an error less than 5.57%. However, experimental data indicate that it is also applicable to large deflections up to 30% within a specific parameter range with an error less than 13.84%.

The main structure of the DSU is a parallel guide beam, which can be customized in size and material. It has a hollow parallel beam segment in the middle that is not thin-walled, and a solid segment at both ends that has a certain thickness. Fig. 2 depicts a simplified force diagram of the DSU in off mode, where a perpendicular force F is applied to the right end tip of a parallel-beam flexure of length L in an x-y coordinate system, with the x-axis oriented horizontally to the right and the y-axis perpendicular to the x-axis downward, and the z-axis is ignored

here. The flexure is divided into three sections, with l_1 and l_3 being solid rigid bodies with moment of inertia I_1 and I_3 respectively, and l_2 being a compliant parallel beam with moment of inertia I_2. The left end of the beam is fixed to the wall.

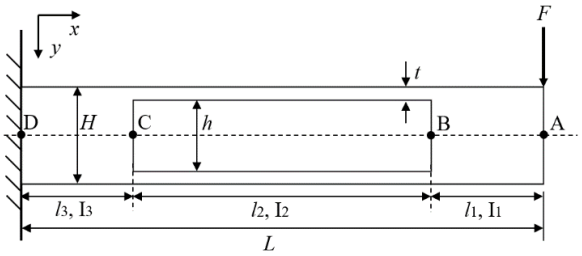

FIGURE 2: FREE BODY DIAGRAM OF THE DSU IN OFF MODE

In Fig. 2, *A*, *B*, *C*, and *D* are located on the center auxiliary line, with A being the stressed end of the flexure, *B* and *C* at the two sections of l_2, and *D* at the fixed end. The height of the flexure is denoted as *H*, and the height of the cavity is *h*. The thickness of a leaf spring in l_2 is $t = (H - h)/2$, and the width *b* is used to calculate the moment of inertia, as shown in the formula:

$$I_1 = I_3 = \frac{H^3 b}{12} \tag{1}$$

$$I_2 = \frac{t^3 b}{12} \tag{2}$$

The flexure is divided into three sections *AB*, *BC*, and *CD* according to l_1, l_2, and l_3. The deflection of the three points *A*, *B*, and *C* are calculated one by one and applied to point *A* to obtain the maximum deflection in the *y*-direction.

First, the *BC* and *BD* sections are treated as rigid, and only the *AB* section is considered. At this point, point *B* can be considered as on the wall, and point *A* is subject to the downward force *F*. The deflection δ_{A1} of point *A* is obtained. where *E* is Young's modulus.

$$\delta_{A_1} = \frac{F l_1^3}{3EI_1} \tag{3}$$

For the *AB* section, the angle of point *A* is not needed to be calculated as it does not affect the final deflection of point *A*. Next, the *AB* and *BD* segments are rigid, and only the *BC* segment is considered. At this point, point *C* can be considered to be on the wall, and point B is subject to the downward force *F* and the bending moment Fl_1 from section *AB*. The deflection angle θ_B of *BC* can be obtained, which will be transmitted to *A* through l_1, causing a deflection δ_{A2} at point *A*. The deflection δ_{A3} of point *B* can be obtained based on the theory of parallel guided mechanisms [20,21].

$$\theta_B = \frac{t^2}{6h^2}\left(\frac{Fl_1 l_2}{EI_2} + \frac{Fl_2^2}{2EI_2}\right) \tag{4}$$

$$\delta_{A_2} = \theta_B l_1 \tag{5}$$

$$\delta_{A_3} = \delta_B = \frac{F l_2^3}{24EI_2} \tag{6}$$

Then, segments *AB* and *BC* are regarded as rigid, and only the segment *CD* is considered. At this time, point *D* is fixed on the wall, and point *C* is affected by the downward force *F* and the bending moment $F(l_1 + l_2)$ from segment *AC*. The force *F* produces an angle θ_{CF} and a deflection δ_{CF}. The moment results in an angle θ_{CM} and a deflection δ_{CM}. The angles cause point *A* to have deflection δ_{A4}. The deflections δ_{CF} and δ_{CM} at point *C* can be transmitted in parallel to point *A*, making point *A* with a deflection δ_{A5}. These parameters are calculated below:

$$\theta_{CF} = \frac{F l_3^2}{2EI_3} \tag{7}$$

$$\delta_{CF} = \frac{F l_3^3}{3EI_3} \tag{8}$$

$$\theta_{CM} = \frac{F(l_1+l_2)l_3}{EI} \tag{9}$$

$$\delta_{CM} = \frac{F(l_1+l_2)l_3^2}{2EI_3} \tag{10}$$

$$\delta_{A_4} = (\theta_{CF} + \theta_{CM})(l_1 + l_2) \tag{11}$$

$$\delta_{A_5} = \delta_{CF} + \delta_{CM} \tag{12}$$

Finally, by adding up all the deflections acting on point A, the maximum deflection δ_A of point *A* under the force *F* and its stiffness k_A are obtained.

$$\delta_A = \delta_{A_1} + \delta_{A_2} + \delta_{A_3} + \delta_{A_4} + \delta_{A_5} \tag{13}$$

$$k_A = \frac{F}{\delta_A} \tag{14}$$

When the DSU is in on mode, the size of the block is set to coincide with the cavity of the beam, and it can be treated as a cantilever beam.

However, considering the limitations of the above model for larger deflections, it is necessary to take other approaches to investigate including all deflection ranges. Machine learning may be a feasible path.

2.3 Training data collection

For data generating, we conduct finite element analysis (FEA) of the parallel beams in ABAQUS by a python script. The 3D beams are automatically generated by several for loops that take several values at equal distances within a certain range in the unit of mm and N. Five values are taken from $l_2 \in [10\ 290]$; four values are taken from $l_1 = l_3 \in [30\ 300 - l_2]$; five values are taken from $H \in [1.4\ l_2]$; five values are taken from $h \in [1\ H - 1.4]$; three values are taken from $b \in [5\ L]$; ten values are taken

from $F \in [0.5\ 100]$. The size of the mesh element increases as the volume of the beam increases with element type C3D20. The material is Al 6061, for which Young's modulus is $E = 6.9\times10^{10}$ Pa and Poisons ratio is 0.33. Finally, 15000 data sets are generated, and takes around 227 hours.

2.4 Machine learning models

In this section, three machine learning-based deflection prediction algorithms SVM, GPR, and MLP are introduced. SVM is a supervised learning model for predicting discrete values, and its fundamental concept is to identify the optimal line of fit. A non-parametric approach for performing regression analysis on data that makes use of a Gaussian process prior is known as Gaussian Process Regression. However, GPR is a computationally expensive technique that is frequently used for solving problems involving low and small sample sizes of regression data. MLP, as demonstrated in Fig. 3, consisting of an input layer, one or more hidden layers, and an output layer, is most notably characterized by multiple neuron layers and is therefore also a deep neural network. Table 1 depicts the MLP model's training process in a straightforward manner.

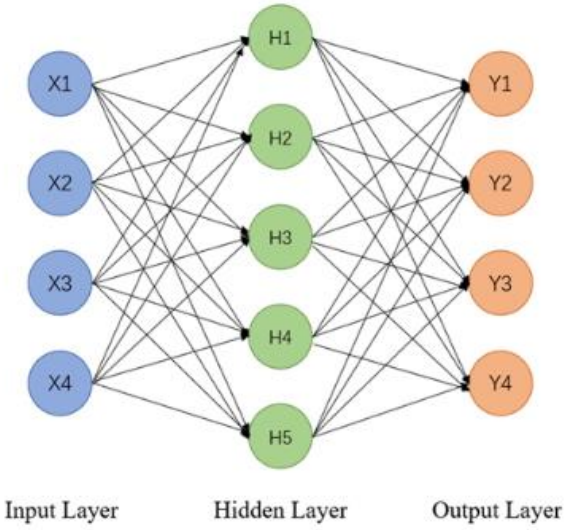

FIGURE 3: AN ILLUSTRATION OF MLP STRUCTURE

In our dataset generated by ABAQUS, the parameters l_1, l_2, l_3, h, H, t, b, F, and δ are included. The other parameters are specified as input besides δ, and the δ values are set as output targets. It should be noted that in order to help the models better grasp the potential connections between the parameters and achieve the best prediction performance, we also use multiple relationship values between the parameters during training. Our dataset contains 15000 data sets, which we divide randomly into a training set having 12500 data sets and a test set involving 2500 data sets. Then we feed the data to three models, let the models be trained and output the deflection values.

TABLE 1. MLP REGRESSION PSEUDOCODE

MLP Regression Pseudocode
1. Set up the original Multi-Layer Perceptron's weights and biases. 2. Set up the training parameters, such as learning rate, epoch number, and batch size. 3. For each epoch: a. Change the order of the training data; b. Separate the data into groups; c. For each batch: i. Send the input through the MLP in reverse order; ii. Use an applicable loss function to figure out the loss; iii. Send the error back through the MLP; iv. Use an optimization algorithm to optimize the weights and biases (e.g., SGD). 4. Estimate the regression performance of the model on a validation set.

3. RESULTS ANALYSIS

3.1 Machine learning performance

We use the collected DSU deflection data to input three chosen regression models, SVM, GPR, and MLP, and assess how well they work. As shown in Table 2, RMSE [22], Error, and Speed are used to compare the effectiveness of three ML models. The higher the quality of the model, the smaller the RMSE value. All three models have extremely low RMSE, indicating that the average difference between the predicted and actual values is minor. In addition, it is demonstrated that the MLP approach has the fastest prediction speed. In light of both prediction accuracy and prediction speed, we believe that MLP is the optimal machine learning technique for predicting the deflection of cantilever beams.

TABLE 2. PERFORMANCE COMPARISON OF ML MODELS

Models	RMSE	Speed (obs /sec)
SVM	0.0025	5.6e+3
GPR	0.0012	1.8e+2
MLP	**0.0012**	**1.2e+4**

3.2 Result comparison

In this Finite Element Analysis (FEA) simulation, we have utilized structural steel as the material of the beam with a Young's modulus of $E = 6.9\times10^{10}$ Pa. The relationship between the stiffness and deflection of the beam with respect to the varying values of h/H has been demonstrated in Fig. 4(a) and Fig. 4(b), respectively. The dimensions of the beam are as follows: $L = 300$ mm, $l_1 = l_3 = 20$ mm, $l_2 = 260$ mm, $H = b = 20$ mm, $F = 10$ N. As anticipated, an increase in h/H results in a reduction in the stiffness and an increase in deflection of the beam. Notably, when h/H equals 0.2, the maximum error of k_A from the

theoretical model relative to the FEA is 11%, whereas the error of the k_{ML} is 0.48%. The overestimation of deflection in the k_{ML} may be due to the lack of specific data samples.

Fig. 4(c) demonstrates the correlation between l_2/L and stiffness, while Fig. 4(d) illustrates the correlation between l_2/L and deflection. In this case, the dimensions of the beam are L = 300 mm, $l_1 = l_3 = (L - l_2)/2$, $H = b$ = 20 mm, F = 10 N. As l_2/L increases, the stiffness of the beam decreases, while the deflection increases. Notably, the three curves are almost coincident. The error of the stiffness k_{ML} compared to the FEA is less than 1.52%, and the error of k_A is always within 2%. The deflection may be underestimated in the k_{ML} formula, which can be explained by the unavoidable factors in the experiments, such as the systematic errors of experimental measurement of our beams.

In Fig. 4(e), the relationship between b/L and stiffness is demonstrated, while Fig. 4(f) illustrates the correlation between b/L and deflection. In this case, the dimensions of the beam are L = 300 mm, $l_1 = l_3$ = 20 mm, l_2 = 260 mm, H = 20 mm, h = 18 mm, F = 10 N. As expected, an increase in b/L leads to an increase in the stiffness of the beam and a decrease in deflection. The error of the stiffness k_A compared to the FEA is always within 5%, while the error of k_{ML} is 1.97%.

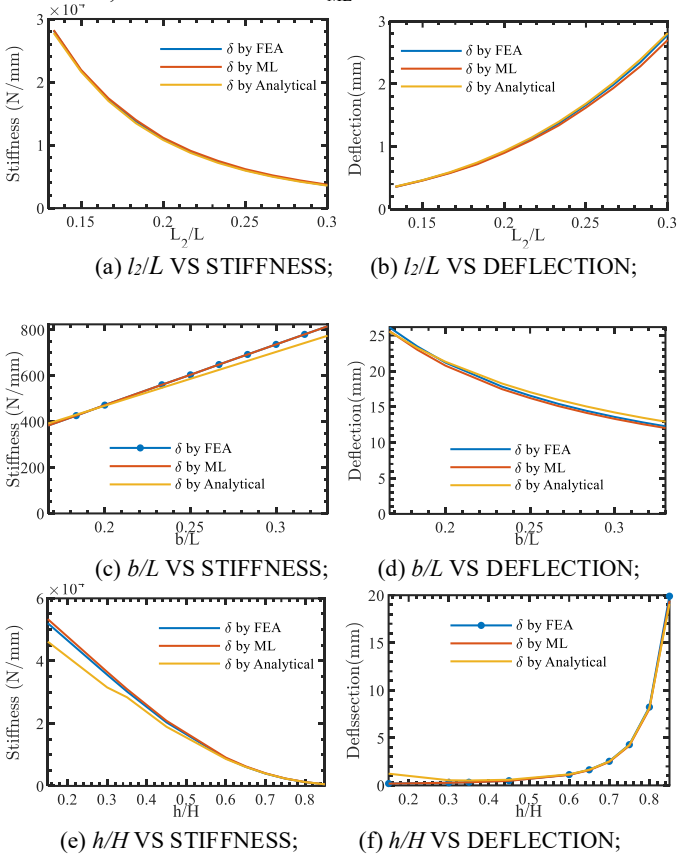

(a) l_2/L VS STIFFNESS; (b) l_2/L VS DEFLECTION;

(c) b/L VS STIFFNESS; (d) b/L VS DEFLECTION;

(e) h/H VS STIFFNESS; (f) h/H VS DEFLECTION;

FIGURE 4: COMPARISON OF THE STIFFNESS OF THE DSU OF FEA, MACHINE LEARNING, AND THEORETICAL VALUE

4. INVERSE DESIGN

One of the main objectives of researchers studying compliant mechanisms is to achieve practical applications. And reverse design is a common method to achieve this goal. The specific approach is to find other reasonable dimensional parameters when the requirements of stiffness and some other dimensional parameters are known. Next, suppose we want to reverse the design of a variable stiffness gripper for a different number of variables. Assume that there are several basic parameters required here regarding the gripper: 1. minimum stiffness K_{min} is 5.36 N/mm; 2. total length L is 100 mm. 3. Material is Al 6061 (E = 69 GPa).

4.3 Case study of one variable

First, the case of finding one parameter unknown is explored. Assuming that F =10 N, $l_1 = l_3$ = 10 mm, H = 20 mm, h = 18 mm, and b = 20 mm are known, the length of the parallel beam l_2 needs to be found. Using MATLAB to solve the existing equation in reverse, we can obtain l_2 = 8 mm. Or use a machine learning approach.

The aforementioned study has proved that our applied algorithms have the ability to release the power of machine learning methods in the linkage of the parallel beam and learning-based regressions. More than this, the deployed methods can lead to a new method for inverse design of size dimensions. Specifically, different from the previous study, we particularly estimate l_2 when giving the other pre-known factors, including K, F, δ, L, l_1, l_3, H, h, and b. When all other factors are fixed, l_2 can be uniquely determined with a result of l_2 = 8.06 mm. And the estimation error RMSE to be 0.026.

4.2 Case study of two variables

Next, the case with two unknown parameters were studied. Assuming that F =10 N, $l_1 = l_3$ = 10 mm, H = 20 mm, and b = 20 mm are known, the length of the parallel beam l_2 and h needs to be found. The rang of l_2 is required from 5 mm to 98 mm, and h is limited from 10 mm to 19 mm. MATLAB is used to solve the relationship between l_2 and h and generate the plot as shown in Fig.5. We can choose a set of l_2 and h from the line in the plot, such as (80 mm, 18 mm). Also, using identical samples as input, and feed them into MLP model, the relationship between l_2 and h. A similar set of l_2 and h can be obtained from the red line in the plot, which (80 mm, 17.96 mm).

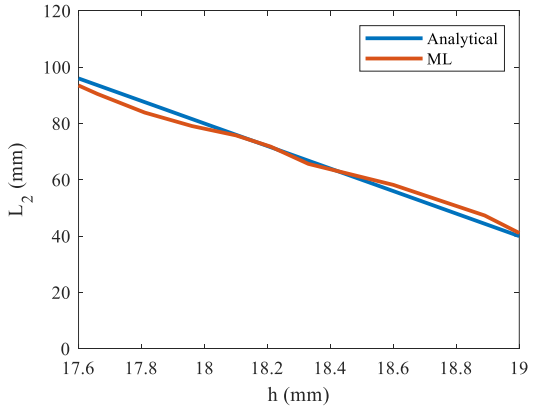

FIGURE 5: FEASIBLE SET OF l_2 AND h

4.3 Case study of three variables

Additionally, we investigated cases involving three unknown parameters. Assuming F =10 N, $l_1 = l_3 = 10$ mm, and $H = 20$ mm are known, we aimed to determine the values of l_2, b, and h for the parallel beam. Specifically, the range of l_2 was required to be between 5 mm to 98 mm, the range of b between 5 mm to 40 mm, and the range of h between 10 mm to 19 mm. We employed MATLAB to solve the relationships between l_2, b, and h, and the resulting plot is presented in Fig. 6. A set of l_2, b, and h can be chosen from the surface in the plot, such as (80 mm, 18 mm, 20 mm).

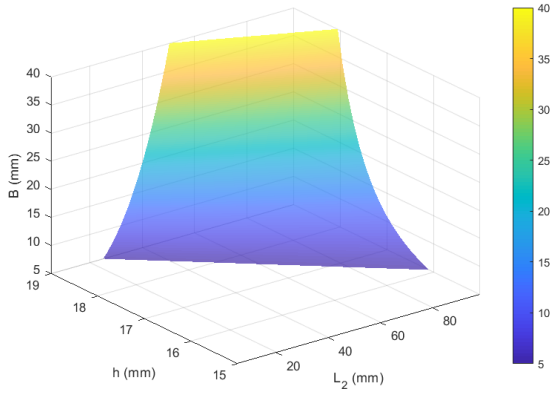

FIGURE 5: FEASIBLE REGION OF l_2, b, AND h

5. CONCLUSIONS

In conclusion, this paper has presented a novel machine learning approach for predicting the deflection of discrete variable stiffness units (DSUs). Three compliant mechanism analysis methods based on machine learning were introduced and compared, and the results showed that these models are faster and more accurate at predicting future outcomes compared to FEA. The study also included a large volume of data collected using FEA under different loads and parameters. An inverse design was implemented, which can predict one or multiple beam parameters gave the other known parameters. While the machine learning algorithm will be improved to increase prediction accuracy, the future goal is to simultaneously predict three or more beam parameters. Overall, this paper presents a certain contribution to the field of compliant mechanism analysis and highlights the potential of machine learning in the area of compliant mechanism.

ACKNOWLEDGMENT

This work is supported by the National Science Foundation (NSF) grant under CMMI-2131711.

REFERENCES

[1] S. Keller et al., An approach of a computerized planning assistant to the system design of collaborative robot installations, *in* IEEE Int. Conf. Emerg. Technol. Fact. Autom. ETFA, *Institute of Electrical and Electronics Engineers Inc.*, (2016).

[2] R. Schiavi, A. Bicchi, and F. Flacco, Integration of active and passive compliance control for safe human-robot coexistence, *in* Proc. - IEEE Int. Conf. Robot. Autom., (2009): pp. 259–264.

[3] K.T. Song, Y.H. Chang, and J.H. Chen, 3D vision for object grasp and obstacle avoidance of a collaborative robot, *in* IEEE/ASME Int. Conf. Adv. Intell. Mechatronics, AIM, *Institute of Electrical and Electronics Engineers Inc.*, (2019): pp. 254–258.

[4] D. Popov, A. Klimchik, and N. Mavridis, Collision detection, localization & classification for industrial robots with joint torque sensors, *in* RO-MAN 2017 - 26th IEEE Int. Symp. Robot Hum. Interact. Commun., *Institute of Electrical and Electronics Engineers Inc.*, (2017): pp. 838–843.

[5] M.I. Awad et al., Passive discrete variable stiffness joint (PDVSJ-II): Modeling, design, characterization, and testing toward passive haptic interface, *J. Mech. Robot.* 11 (1) (2019).

[6] D. Rus and M.T. Tolley, Design, fabrication and control of soft robots, *Nat. 2015 5217553* 521 (7553) (2015) 467–475.

[7] D. Gan et al., Stiffness design for a spatial three degrees of freedom serial compliant manipulator based on impact configuration decomposition, *J. Mech. Robot.* 5 (1) (2013) 11002-1-11002–10.

[8] L.L. Howell and A. Midha, Parametric Deflection Approximations for End-Loaded, Large-Deflection Beams in Compliant Mechanisms, *J. Mech. Des.* 117 (1) (1995) 156–165.

[9] H.J. Su, A pseudorigid-body 3r model for determining large deflection of cantilever beams subject to tip loads, *J. Mech. Robot.* 1 (2) (2009) 1–9.

[10] F. Ma and G. Chen, Modeling large planar deflections of flexible beams in compliant mechanisms using chained beam-constraint-model, *J. Mech. Robot.* 8 (2) (2016).

[11] D. Lai, C. Demartino, and Y. Xiao, Interpretable machine-learning models for maximum displacements of RC beams under impact loading predictions, *Eng. Struct.* 281 (2023) 115723.

[12] J. Fu and D. Gan, A Reconfigurable Variable-Stiffness Parallel Beam for Compliant Robotic Mechanisms Towards Safe Human Interaction, *Proc. ASME Des. Eng. Tech. Conf.* 8A-2021 (2021).

[13] M. Trojanová, A. Hošovský, and T. Čakurda, Evaluation of Machine Learning-Based Parsimonious Models for Static Modeling of Fluidic Muscles in Compliant Mechanisms, *Math. 2023, Vol. 11, Page 149* 11 (1) (2022) 149.

[14] Y. Jin and H.J. Su, Machine Learning Models for Predicting Deflection and Shape of 2D Cantilever Beams, *Proc. ASME*

Des. Eng. Tech. Conf. 7 (2022).
[15] E. Schulz, M. Speekenbrink, and A. Krause, A tutorial on Gaussian process regression: Modelling, exploring, and exploiting functions, *J. Math. Psychol.* 85 (2018) 1–16.
[16] J. Lim, S. Ha, and J. Choi, Prediction of Reward Functions for Deep Reinforcement Learning via Gaussian Process Regression, *IEEE/ASME Trans. Mechatronics* 25 (4) (2020) 1739–1746.
[17] D.T. Pham and S. Sagiroglu, Training multilayered perceptrons for pattern recognition: a comparative study of four training algorithms, *Int. J. Mach. Tools Manuf.* 41 (3) (2001) 419–430.
[18] I. Hussain et al., Modeling, identification, and control of a discrete variable stiffness actuator (DVSA), *Actuators* 8 (3) (2019).
[19] J. Fu et al., A Novel Variable Stiffness Compliant Robotic Link Based on Discrete Variable Stiffness Units for Safe Human–Robot Interaction, *J. Mech. Robot.* 16 (1) (2024).
[20] S. Awtar, K. Shimotsu, and S. Sen, Elastic averaging in flexure mechanisms: A three-beam parallelogram flexure case study, *J. Mech. Robot.* 2 (4) (2010).
[21] L.L. Howell, S.P. Magleby, and B.M. Olsen, *Handbook of Compliant Mechanisms*, *Wiley*, (2013).
[22] T. Chai and R.R. Draxler, Root mean square error (RMSE) or mean absolute error (MAE)? -Arguments against avoiding RMSE in the literature, *Geosci. Model Dev.* 7 (3) (2014) 1247–1250.